Cavitation selectively reduces the negative-pressure phase of lithotripter shock pulses

Yuri A. Pishchalnikov
Department of Anatomy and Cell Biology, Indiana University School of Medicine, 635 Barnhill Drive, Indianapolis, IN 46202
yura@anatomy.iupui.edu

Oleg A. Sapozhnikov
Department of Acoustics, Physics Faculty, M.V. Lomonosov Moscow State University, Moscow 119992, Russia
oleg@acs366.phys.msu.ru

Michael R. Bailey
Center for Industrial and Medical Ultrasound, Applied Physics Laboratory, University of Washington, Seattle, WA 98105
bailey@apl.washington.edu

Irina V. Pishchalnikova, James C. Williams, Jr., and James A. McAteer
Department of Anatomy and Cell Biology, Indiana University School of Medicine, 635 Barnhill Drive, Indianapolis, IN 46202
irina@anatomy.iupui.edu; williams@anatomy.iupui.edu; mcateer@anatomy.iupui.edu

Abstract: Measurements using a fiber-optic probe hydrophone, high-speed camera, and B-mode ultrasound showed attenuation of the trailing negative-pressure phase of a lithotripter shock pulse under conditions that favor generation of cavitation bubbles, such as in water with a high content of dissolved gas or at high pulse repetition rate where more cavitation nuclei persisted between pulses. This cavitation-mediated attenuation of the acoustic pulse was also observed to increase with increasing amplitude of source discharge potential, such that the negative-pressure phase of the pulse can remain fixed in amplitude even with increasing source discharge potential.

© 2005 Acoustical Society of America
PACS numbers: 43.35.Ei, 43.80.Gx, 43.25.Yw, 43.25.Vt [TM]
Date Received: June 10, 2005 **Date Accepted:** November 1, 2005

1. Introduction

It has been shown that cavitation bubbles produced by a lithotripter shock pulse can play a role in stone breakage and tissue damage (reviewed in Ref. 1). Recent publications suggest that cavitation can also affect the propagation of the acoustic pulse *in vitro*[2,3] and *in vivo*.[4] Experiments in Ref. 2 demonstrated that waveforms recorded in the focus of a piezoelectric transducer, which is expected to have very repeatable signals, can show significant fluctuations after the first tensile phase of the wave. It was suggested that these fluctuations, which start approximately at the tensile maximum, were caused by propagation effects and, in particular, by cavitation bubble activity. This hypothesis was verified by comparison of recorded signals in water having different cavitation conditions: tap water, degassed water, and water containing acetic acid used to dissolve calcite crystals that can retain minute bubbles. Experimental results were confirmed by numerical simulation, which showed that with increasing bubble number density the tensile part of the acoustic pulse was shorter, and was followed by noticeable secondary oscillations.[2]

In the present study we attempted to understand why cavitation bubbles selectively reduce the trailing negative-pressure phase of the lithotripter pulse without affecting much the leading positive-pressure phase of the same pulse. Pulse repetition frequency (PRF) was used to seed the field with cavitation nuclei,[5] and studies were performed at PRFs in the clinical range

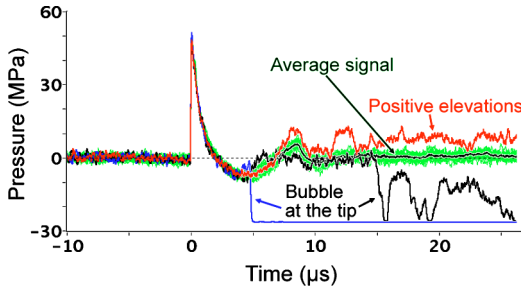

Fig. 1. A series of 25 consecutive pulses recorded with FOPH at the geometric focus of the DoLi-50 lithotripter (L6, 0.5 Hz). Undistorted signals are shown by 22 superimposed green traces, with the average waveform shown by the dark green line. Signals distorted by cavitation at the tip or along the surface of the optical fiber are shown by blue, black, and red traces.

(0.5–2 Hz) using clinical electrohydraulic and electromagnetic lithotripters. We observed that cavitation restricts the energy delivered by the negative-pressure phase of the pulse, such that, in the presence of cavitation, a further increase in charging potential of the lithotripter does not necessarily provide a corresponding increase in the negative-pressure phase of the pulse. These findings show how readily the tensile phase of the shock pulse is affected by cavitation, and help explain why it is so difficult to use the features of the tensile phase to characterize the acoustic output of shock wave lithotripters.

2. Methods

Measurements were conducted in an unmodified Dornier HM3 electrohydraulic lithotripter, a research lithotripter patterned after the HM3 (HM3-clone),[6] and a Dornier DoLi-50 electromagnetic lithotripter (Dornier MedTech Systems, Germany). The HM3 and HM3-clone lithotripters have their own water-processing systems, while tap water in the test tank of the DoLi-50 was degassed using a pinhole system.[7] The gas content of water was measured using a WTW Oxi 330i oxygen meter (Weilheim, Germany). In the DoLi-50 tank the oxygen content was about 4 mg/l, or 50% of saturation. In the HM3, fresh degassed water (4%–7% of saturation) is continuously pumped into the bottom of the bath, while excess water is removed via an overflow drain. When the circulation system was turned off, the oxygen content of the water slowly increased from its dynamic equilibrium value of ~8% to reach ~25% by 2.5 h. During this period, the water temperature dropped from 39.7 °C to ~36 °C. Measurements with the HM3-clone and the DoLi-50 were conducted at room temperature (~22 °C). The effect of temperature was not investigated in this study.

Waveforms were measured at the focus of each lithotripter using a fiber-optic probe hydrophone FOPH-500 (University of Stuttgart, Germany).[8] It has been reported that the fiber-optic hydrophone, because of the strong adhesion of water to glass, is resistant to the cavitation artifacts (i.e., reduced amplitude of negative pressure) that typically affect PVDF hydrophones.[8] However, FOPH signals are not free of artifacts. Three examples of aberrant signals are given in Fig. 1, which shows 25 consecutive shock waves (SWs) recorded in the DoLi-50. In the two signals marked by blue and black traces, cavitation bubbles at the fiber tip created an optical mismatch (as the refractive index of the gas is dramatically different from water) that produced a strong negative spike in the FOPH signal.[8] A trace marked in red shows several positive elevations, probably caused by bubbles along the fiber cable. We hypothesize that cavitation along the fiber cable could deform the fiber and thereby deflect the light. Distortions were seen to be more pronounced in strong acoustic fields and under conditions where bubbles formed easily on the surface of the fiber. Such aberrant waveforms (see the examples in Fig. 1), in which the acoustic pressure did not return to baseline after passage of the pulse, were easily distinguished from typical waveforms, and were excluded from the analysis (see below).

 1529-7853/2005/6(4)/280/7/$0.00 © 2005 Acoustical Society of America

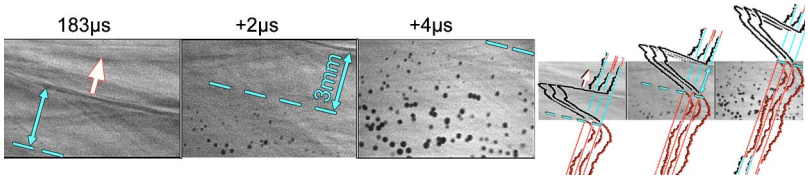

Fig. 2. Three frames of high-speed shadowgraph photography taken during the passage of a shock pulse through the focal region of the HM3-clone lithotripter. Shadow of the shock front is seen at the center of the first frame (183-μs delay) with the direction of pulse propagation shown by the single arrow ($F2$ is at the base of the single arrow). On the second frame (+2 μs) the shock front is seen at the top right corner, with the position of the previous shock front shown by a blue dashed line. During the 2-μs time step between frames, the shock front traveled 3 mm, which is depicted by a blue double-headed arrow between the shock front and its previous position (dashed line). Since the duration of the positive-pressure phase of the pulse is ~2 μs, the dashed line also marks the transition from positive to negative acoustic pressure, so that the double-headed arrow shows the region occupied by the positive-pressure phase of the pulse. In the third frame (+4 μs) the dashed line is at the right top corner; thus, the positive-pressure phase has already passed, and the frame is occupied by the negative-pressure tail. Note that the tensile stress gives rise to the growth of cavitation bubbles (which appear black), so that the rest of the negative tail propagates through a more "bubbly" liquid. The diagram to the right shows three temporal profiles (recorded at the focal plane at −1, 0, and +1 mm relative to $F2$) superimposed atop the high-speed (HS-camera) images. The measured negative-pressure phase (highlighted by red) lasts for ~6 μs, corresponding to a distance of 9 mm (3 times longer than the positive-pressure region shown by the double-headed arrow).

Waveforms were typically collected in sets of 100 pulses using the Fast Frame setup of the Tektronix (TDS 5034) oscilloscope, with a 1–3-min interval between each series to check the sensitivity of the FOPH. Postprocessing of the recorded data was performed with programs written in LabVIEW (National Instruments, Austin, TX). Averaged waveforms were calculated by aligning recorded pulses to the coincidence of the half amplitude of the shock fronts.

Cavitation bubbles were visualized with B-mode ultrasound and high-speed photography. The B-mode ultrasound system (Terason 2000, Burlington, MA) employed a curved linear probe (4C2 wideband, 128 element) with 4-MHz center frequency. The appearance of echogenic regions that brighten and fade coincident with the lithotripter PRF are interpreted as scattering from bubble clouds. Previously these echogenic regions have been shown to be the locations of passive cavitation signals.[4] To enable studies with a high-speed camera (HS-camera), the water tank of the HM-3 clone was made of optically clear acrylic.[1] The HS-camera (Imacon 468, DRS Hadland, Inc., Cupertino, CA) could record seven 576×385-pixel frames with a maximum speed of 100 million frames per second.

In selected HS-camera experiments, pre-existing bubbles were created in the focal region of the HM3-clone lithotripter. An uncapped, air-filled 15-ml polyethylene centrifuge tube was positioned mouth-down, 1 cm above $F2$ (out of the field of view in Mm.3). Air was pulled from the tube with each pulse, creating a dense bubble cloud at $F2$. Some of these air-filled bubbles persisted in the focal region until the next lithotripter pulse delivered at 2 Hz.

3. Results

Shadowgraph photography was used to observe passage of the lithotripter shock pulse and the appearance of cavitation bubbles. Figure 2 shows three HS-camera frames recorded with a 2-μs step encompassing the arrival of the shock wave at the $F2$ focus of the HM3-clone lithotripter. The shadow of the shock front is seen on the first and second frames (183 μs, +2 μs), and the transition from positive to negative pressure is marked by a dashed line. Formation and subsequent growth of cavitation bubbles is seen in the second and third frames (+2 μs, +4 μs). Bubbles become visible slightly below the dashed line, that is, soon after the transition from positive to negative pressure. Thus, shadowgraph photography demonstrates that the trailing negative-pressure phase of the lithotripter shock pulse propagates through more bubbles than the leading positive-pressure phase of the same pulse.

The population density of cavitation bubbles varied from pulse to pulse and in general increased with pulse amplitude, gas saturation of the water, and pulse repetition rate. The HS-

 1529-7853/2005/6(4)/280/7/$0.00 © 2005 Acoustical Society of America

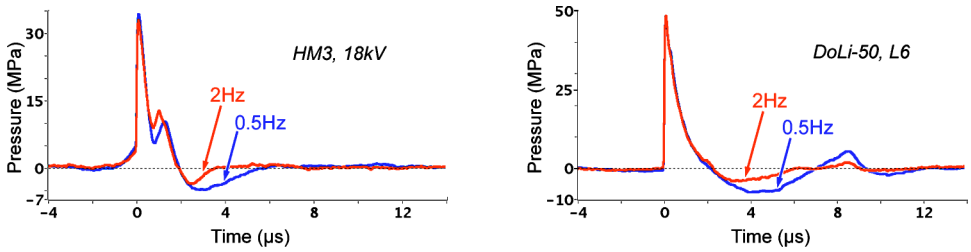

Fig. 3. Effect of PRF on waveforms generated by an electrohydraulic lithotripter (Dornier HM3, left) and an electromagnetic lithotripter (Dornier DoLi-50, right). In the HM3, the amplitude and duration of the negative-pressure phase is reduced at 2 Hz compared to 0.5 Hz. (Note: The positive-pressure phase of the HM3 pulse has double-peak structure caused by superposition of the edge waves.) The waveforms for the DoLi-50 (right) also show truncation of the negative-pressure phase at faster PRF. In addition, trailing oscillations seen here (starting at ~7 μs) are also suppressed at faster PRF. Each waveform is an average of 100 pulses.

camera sequence shown in Fig. 2 captured the passage of the fifth lithotripter pulse (HM3-clone) administered at 2 Hz (20 kV) in water degassed to about 50% of saturation. In more thoroughly degassed water, dense bubble clouds (similar to that shown in Fig. 2) could be generated by delivering lithotripter pulses at a faster pulse repetition frequency (PRF) of ~3–5 Hz. For example, Mm. 1 shows the growth and collapse of a bubble cloud generated by the tenth shock wave administered at 5 Hz (20 kV) in water with ~20% saturation. The first frame was captured 10 μs prior to the arrival of the shock front at $F2$. The second frame was recorded 130 μs later and shows numerous cavitation bubbles that continue their inertial growth long after the passage of the lithotripter pulse. About 800 μs after the passage of the lithotripter pulse, the bubble cloud has disappeared. In Fig. 2 and Mm.1 there are no visible bubbles remaining from the previous pulses. This is not surprising because the growth-collapse cycle for cavitation bubbles is several hundred microseconds long (Mm.1), which is roughly 1000 times shorter than the pulse interval. In spite of the short lifespan of visible bubbles, the HS-camera typically registered more cavitation bubbles generated by lithotripter pulses delivered at faster PRF. This suggests that some cavitation nuclei (microscopic bubbles) persisted at faster PRF, but these nuclei were below the resolution of the HS-camera ($<$50 μm in radius).

Mm.1. High speed-camera (HS-camera) movie of the growth-collapse cycle of cavitation bubbles (0.8 Mb).

Unlike bubbles visible by the HS-camera, echo from cavitation bubbles detected by B-mode ultrasound persisted for a much longer period (resonant bubble size is on the order of only a few μm). Mm. 2 shows three seconds of ultrasound imaging (displayed in slow motion) recorded in the focal plane of the DoLi-50, and catches six shock waves delivered at 2 Hz. Though most of the echo disappeared between pulses (most nuclei were already below the resolution of the B-mode ultrasound), the size and position of the cloud of nuclei can be tracked. At this PRF and gas content some nuclei persist until the arrival of the next lithotripter pulse. Mm.2 also demonstrates that the cloud of nuclei can dramatically change its shape and position from pulse to pulse, and that nuclei remaining within the focal area determine the size and position of the bubble cloud generated by the next pulse.

Mm.2(a) B-mode ultrasound in the focal region of the DoLi-50 at 2 Hz (1.5 Mb).

Mm.2(b) MPEG-4 version (lower quality) of Mm.2(a) if you have difficulty playing Mm2(a) (1.5 Mb).

At higher PRF, more cavitation nuclei persist between pulses. This gives rise to bubble clouds that are more dense, causing greater attenuation of the negative-pressure phase of the pulse. Figure 3 compares pulses at 2 and 0.5 Hz for electrohydraulic (left panel) and electromagnetic (right panel) lithotripters. Since initially cavitation nuclei occupy only a small void fraction, they have little effect on the leading compressive phase of the pulse. However, these

 1529-7853/2005/6(4)/280/7/$0.00 © 2005 Acoustical Society of America

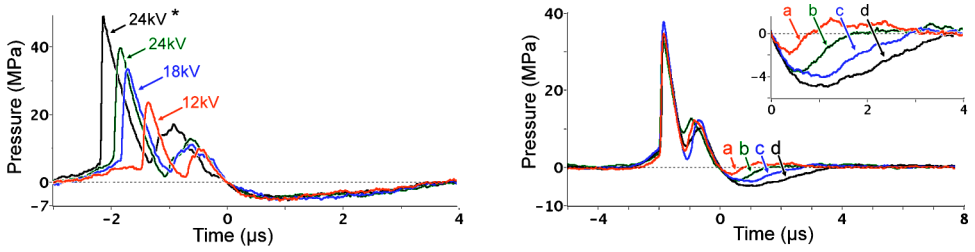

Fig. 4. Left panel—Effect of charging potential on Dornier HM3 waveforms. Amplitude of the positive-pressure phase increases as kV is increased, but the negative-pressure phase is unaffected. It is likely that this occurs because cavitation is greater at higher kV, and the growth of more and larger bubbles pulls additional energy from the pulse, leading to saturation of its negative-pressure phase. Each waveform is an average of 10 pulses recorded at 1 Hz. Right panel—Effect of gas content on Dornier HM3 waveforms. Increasing the gas content of the water reduces the amplitude and duration of the negative-pressure phase: (a) 25% oxygen saturation at 2 Hz; (b) 8% saturation at 2 Hz; (c) 25% saturation at 0.5 Hz; and (d) 8% saturation at 0.5 Hz. The inset is an enlargement of the negative tail. Zero time is positioned at the transition point from positive to negative acoustic pressure. Each waveform is an average of 100 pulses recorded at 18 kV.

nuclei seed the growth of bubbles under the influence of the trailing tensile phase of the pulse (Fig. 2), which leads to the more pronounced attenuation of the negative tail observed for pulses at 2 Hz (Fig. 3).

In the HM3 and HM3-clone electrohydraulic lithotripters, the spark discharge generates bubbles that drift away from the path of the shock wave. However, the faster the PRF, the more bubbles are present along this path. Spark-generated bubbles may be responsible for the modest drop in peak positive pressure at 2 Hz compared to 0.5 Hz shown in Fig. 3 (left panel). To study pulse propagation through pre-existing bubbles, bubbles were "artificially" created at the focal area of the HM3-clone lithotripter using an inverted centrifuge tube (please see Sec. 2). Mm.3 shows the passage of the fifth lithotripter pulse administered at 2 Hz (20 kV). The leading positive-pressure phase of the pulse suppressed and collapsed pre-existing bubbles, causing them to radiate spherical shock waves. Note also that, similar to Fig. 2, arrival of the tensile stress (behind the dashed line, Mm.3) gives rise to the growth of numerous cavitation bubbles, so that the leading positive-pressure wave and the trailing negative-pressure phase of the same pulse propagate through different amounts of "bubbliness" of the liquid. Thus, with or without pre-existing bubbles, the negative-pressure phase is attenuated much more than the leading positive wave, though bubbles that persist prior to the arrival of the pulse can reduce the amplitude of the positive wave as well.

Mm.3. Shock pulse propagation in water with pre-existing bubbles (1.3 Mb).

Acoustic pulses generated by electromagnetic lithotripters show fast-fading oscillations that trail the negative-pressure phase of the pulse (Fig. 3, right panel). These oscillations, caused by electric current oscillation between the coil and capacitor,[9] propagate through cavitation bubbles generated by the negative-pressure phase. The momentum delivered by the leading (most noticeable) positive "bump" of these oscillations can be sufficient to collapse small bubbles, and to slow down the growth of larger bubbles. These oscillations were found to be more attenuated at 2 Hz than at 0.5 Hz (Fig. 3, right panel), correlating with the presence of more cavitation bubbles at higher PRF.

In general, increasing the charging potential of the lithotripter increases cavitation. However, the higher the density of cavitation bubbles, the greater the attenuation of the negative tail. This may lead to a slowdown in the growth of the negative pressure or even to its "saturation." The left panel in Fig. 4 illustrates pulses measured at different voltage settings, and shows that the increase in positive pressure was not accompanied by an increase in the negative tail. Shock waves were generated with a new electrode, which produced more consistent waveforms. The black waveform (24 kV*) was recorded with the electrode preconditioned by 400 pulses administered at 18 kV, thus yielding a larger amplitude. Though the peak positive pressure and

the duration of the positive-pressure phase both increased with voltage settings, the negative tail was unchanged (saturated). At the same time, even at the same voltage settings, the amplitude and duration of the negative-pressure phase of lithotripter shock pulses can strongly depend on the density of cavitation bubbles (Fig. 4, right panel). In addition to the effect of PRF on the negative tail, truncation of the negative-pressure phase was observed when water circulation in the HM3 bath was turned off, and the content of the dissolved gas was allowed to increase (compare waveforms at the same PRF: (a) vs (b), and (c) vs (d). As already discussed, peak positive pressure at 2 Hz (a) and (b) was slightly less than corresponding values at 0.5 Hz (c) and (d), respectively). Figure 4 underscores the importance of taking into account cavitation phenomena, as bubbles can change the waveform and noticeably reduce the negative pressure.

4. Discussion and conclusions

These results show that bubble growth generated by the trailing negative-pressure phase of a lithotripter shock pulse attenuates the tail of the very same pulse. This appears to occur because the momentum for expansion of bubbles is withdrawn from the acoustic pulse, such that the lithotripter pulse loses energy. This energy no longer belongs to (travels with) the pulse, but is left in the medium in the form of kinetic and potential energy of the liquid surrounding the bubbles. The energy needed for a solitary cavitation bubble to grow to its maximum radius R_{max} is proportional to R_{max}^3, and for $R_{max}=0.5$ mm is about 0.05 mJ.[10] The total energy of the negative tail, for the HM3 pulses shown in the left panel of Fig. 3, is about 8 mJ for 0.5-Hz pulses and 1.6 mJ for 2-Hz pulses (energy was calculated using the temporal profile of the pulse and a measured radius of 1 cm for the half amplitude of the negative pressure). Thus, if the lower negative tail energy in the 2-Hz pulse were due entirely to loss of energy to bubble formation, one would predict the generation of about 100 more bubbles with $R_{max}=0.5$ mm (or 1000 bubbles with $R_{max}=0.25$ mm) with the 2-Hz pulse than with the 0.5-Hz pulse. This number of bubbles seems reasonable from the high-speed photography data (Fig. 2, Mm1). Thus, the decrease in negative tail energy with increased rate of pulse application can be attributed to loss of energy into bubble growth.

Attenuation of the negative-pressure phase of the lithotripter pulse only occurred when cavitation bubbles formed (i.e., a threshold phenomenon), and was more pronounced in strong cavitation fields. Hydrophone measurements indicate that the attenuation was initiated within 1 μs of arrival of the negative wave, contemporaneous with the first observation of expanding bubbles by high-speed photography. As cavitation bubbles grew, they increasingly affected propagation of the negative wave, reducing its amplitude and duration. When cavitation was minimal, the positive and negative pressure phases of the pulse temporal profile typically had the same area. We observed, however, that reduction of the tensile stresses by cavitation could upset this balance, making the positive area much higher than the negative area (Fig. 4).

Higher PRF was used to increase the number of cavitation bubbles, which appeared to be due to persistence of cavitation nuclei (microscopic bubbles) that did not have enough time to dissolve between pulses (Mm.2,[5,11]). These small cavitation nuclei had little effect on the leading compressive wave, but seeded the growth of bubbles under the influence of the tensile wave (Fig. 2. and Mm.3). Consistent with more cavitation bubbles typically observed by HS-camera and B-mode ultrasound at higher PRF, reduced negative pressure was observed at 2 Hz compared to 0.5 Hz (Fig. 3). Truncation of the negative tail was not observed in filtered, well-degassed water at low power levels, but became noticeable as the power level was increased—correlating with higher bubble densities in the cloud.

Loss of acoustic energy into expansion of cavitation bubbles restricts the amount of energy delivered by the negative-pressure phase of the pulse. That is, failure (or rupture) of liquid under tensile stresses (i.e., bubble formation) imposes a limit on the amplitude of the negative pressure that can be transmitted through water. The rationale is that a more prominent negative tail generates a higher density of cavitation bubble clouds which, in turn, causes stronger dissipation of the pulse. As the negative-pressure phase of the pulse becomes smaller, the effectiveness of bubble generation will be diminished, so that further dissipation of the pulse

 1529-7853/2005/6(4)/280/7/$0.00 © 2005 Acoustical Society of America

energy is reduced. This mechanism may lead to a kind of self-regulated stabilization or "saturation" of the negative-pressure phase, as observed in Fig. 4 (left panel).

The observation that cavitation can have a dramatic effect on the amplitude and duration of the negative-pressure phase of the lithotripter pulse may well have implications that have yet to be fully appreciated. With the advent of hydrophones that provide a better rendition of negative pressure, one expectation is that it should be possible to determine values of the tensile phase with greater confidence. However, our findings, and those of others,[2,3] show that the amplitude of the negative pressure phase is very sensitive to cavitation. Thus, before values for negative pressure can become a routine feature of the characterization of lithotripters, more attention needs to be paid to the conditions under which measurements are performed.

Acknowledgments

The authors thank Richard J. VonDerHaar for assistance during FOPH measurements, Philip Blomgren for his useful technical advice, and Dr. Bret Connors for help in work with the HM3. This work was supported by grants from the National Institutes of Health (DK-43881) and ONRIFO.

References and links

[1]Y. A. Pishchalnikov, O. A. Sapozhnikov, M. R. Bailey, J. C. Williams, Jr., R. O. Cleveland, T. Colonius, L. A. Crum, A. P. Evan, and J. A. McAteer, "Cavitation bubble cluster activity in the breakage of kidney stones by lithotripter shockwaves," J. Endourol **17**(7), 435–446 (2003).

[2]M. Liebler, T. Dreyer, and R. E. Riedlinger, "Focal Pressure Variations in Shock Wave Therapies Caused by Cavitation Bubbles," Proc. of the Joint Congress CFA/DAGA'4, 983–984 (2004); http://www.ihe.uni-karlsruhe.de/forschung/akustik/Paper_Liebler_DAGA04.pdf

[3]G. N. Sankin, "Luminescence induced by spherically focused acoustic pulses in liquids," Acoust. Phys. **51**, 338–346 (2005).

[4]M. R. Bailey, Y. A. Pishchalnikov, O. A. Sapozhnikov, R. O. Cleveland, J. A. McAteer, N. A. Miller, I. V. Pishchalnikova, B. A. Connors, L. A. Crum, and A. P. Evan, "Cavitation detection during shock wave lithotripsy," Ultrasound Med. Biol. **31**(9), 1245–1256 (2005).

[5]O. A. Sapozhnikov, V. A. Khokhlova, M. R. Bailey, J. C. Williams, Jr., J. A. McAteer, R. O. Cleveland, and L. A. Crum, "Effect of overpressure and pulse repetition frequency on cavitation in shock wave lithotripsy," J. Acoust. Soc. Am. **112**(3), 1183–1195 (2002).

[6]R. O. Cleveland, M. R. Bailey, N. Fineberg, B. Hartenbaum, M. Lokhandwalla, J. A. McAteer, and B. Sturtevant, "Design and characterization of a research electrohydraulic lithotripter patterned after the Dornier HM3," Rev. Sci. Instrum. **71**, 2514–2525 (2000).

[7]A. R. Kaiser, C. A. Cain, E. Y. Hwang, J. B. Fowlkes, and R. J. Jeffers, "A cost effective degassing system for use in ultrasonic measurements: The multiple pinhole degassing system," J. Acoust. Soc. Am. **99**(6), 3857–3859 (1996).

[8]J. Stardenraus and W. Eisenmenger, "Fiber-optic probe hydrophone for ultrasonic and shock-wave measurements in water," Ultrasonics **31**, 267–273 (1993).

[9]W. Eisenmenger, "Electromagnetic generation of plane pressure pulses in liquids," (In English) and "Electromagnetische erzeugung von ebenen druckstossen in flussigkeiten," (In German), Acustica **12**, 185–201 (1962).

[10]P. Zhong, Y. F. Zhou, and S. L. Zhu, "Dynamics of bubble oscillation in constrained media and mechanisms of vessel rupture in SWL," Ultrasound Med. Biol. **27**(1), 119–134 (2001).

[11]M. Arora, L. Junge, and C. D. Ohl, "Cavitation cluster dynamics in shock-wave lithotripsy. I. Free field," Ultrasound Med. Biol. **31**, 827–839 (2005).

 1529-7853/2005/6(4)/280/7/$0.00 © 2005 Acoustical Society of America